

The characteristics of dose at mass interface on lung cancer Stereotactic Body Radiotherapy (SBRT) simulation

I H Wulansari¹, W E Wibowo² and S A Pawiro¹

¹Departement of Physics, Faculty of Mathematics and Natural Sciences, Universitas Indonesia, Depok, West Java, 16424, Indonesia

²Radiotherapy Departement, National General Hospital Cipto Mangunkusumo, Jakarta, 10430, Indonesia.

E-mail: supriyanto.p@sci.ui.ac.id

Abstract. In lung cancer cases, there exists a difficulty for the Treatment Planning System (TPS) to predict the dose at or near the mass interface. This error prediction might influence the minimum or maximum dose received by lung cancer. In addition to target motion, the target dose prediction error also contributes in the combined error during the course of treatment. The objective of this work was to verify dose plan calculated by adaptive convolution algorithm in Pinnacle³ at the mass interface against a set of measurement. The measurement was performed using Gafchromic EBT 3 film in static and dynamic CIRS phantom with amplitudes of 5 mm, 10 mm, and 20 mm in superior-inferior motion direction. Static and dynamic phantom were scanned with fast CT and slow CT before planned. The results showed that adaptive convolution algorithm mostly predicted mass interface dose lower than the measured dose in a range of -0,63% to 8,37% for static phantom in fast CT scanning and -0,27% to 15,9% for static phantom in slow CT scanning. In dynamic phantom, this algorithm was predicted mass interface dose higher than measured dose up to -89% for fast CT and varied from -17% until 37% for slow CT. This interface of dose differences caused the dose mass decreased in fast CT, except for 10 mm motion amplitude, and increased in slow CT for the greater amplitude of motion.

1. Introduction

In radiotherapy planning, it is difficult for the Treatment Planning System (TPS) to predict the dose at or near mass interface. These are caused by the loss of lateral or longitudinal electronic equilibrium [1]. The TPS commonly uses dose correction methods to compensate the dose change in photon fluence, but the changes in charged particle transport to calculate the inhomogeneity is not taken into account [2]. TPS inaccuracies in predicting the interface dose causes a discrepancy between TPS dose calculations and the experimental results; there was an underdose at mass lung interface [3].

Measurements of lung SBRT doses during the procedure is deemed complicated to be performed owing to the inclusion of some factors such as tissue density differences, charged particle disequilibrium in the small field, and motion of the lungs. Moreover, dosimetry complexity is also caused by the beam passing through the difference of material densities [4]. In addition, the effect of the materials density difference was exacerbated by the presence of charged particle disequilibrium (CPD) on a small field in SBRT [5]. However, Treatment planning system (TPS) with a simple calculation algorithm generally did not calculate this effect [3]. This can lead to overdose or underdose in contrast to the actual dose received by patients. In addition, the motion of the lungs might also influence the accuracy of the radiation beam delivery [6], [7].



In this work, dose measurement in mass lung interface with a static and dynamic condition is presented. The lung mass was irradiated with 6 MV photon beam and compared to TPS Pinnacle³ with adaptive convolution algorithm. The aim of this work was to identify the TPS tendency of predicting dose of mass interface and to identify underdose degree in the interface region.

2. Materials and Methods

Simulation of lung cancer has been created using CIRS phantom 002FLC with cylindrical acrylic of 2.9 cc volume to simulate the cancer target. The simulated target cancer was introduced to the left lung as seen in Figure 1. The phantom, with target, was scanned using helical CT with fast and slow CT techniques. The scanning time were 1 second per slice and 2 seconds per slice for fast and slow CT techniques, respectively. The phantom was scanned in a static and dynamic setup in the superior-inferior direction with the amplitudes of the phantom motion were of 5 mm, 10 mm and 20 mm to represent the lung motion. The dynamic setup was managed by CIRS phantom 002FLC using phantom motion control 008PL. The acquired images were sent to the TPS to simulate SBRT forward planning. Contouring of simulated cancer mass as clinical target volume (CTV) was performed on both images from fast and slow CT scanning in a static and dynamic setup. The gross target volume (GTV) has a margin of 2 mm for CTV, whereas the planning target volume (PTV) was arranged with an error margin of 2 mm from GTV. 15 beams were arranged around the cancer mass with 80% prescription dose of 6000 cGy in 12 fractions on GTV. Afterwards, the planning was exported to Synergy S linear accelerator for 6 MV photon beam delivery. To ensure the positioning accuracy of the measurements, isocenter position was verified using CBCT and room laser.

For measurements, the dose in the interface cancer was measured using Gafchromic EBT3. It was calibrated with source axis distance (SAD) 100 cm, filed size of 10 x10 cm² in solid water phantom with dose in the range of 0 to 1800 cGy. The irradiated films were scanned using EPSON V700 of 72 dpi resolution and saved in .TIF format. In order to determine the dose distribution and point dose of interface cancer, the scanned film was read using in-house dose verification (IDV) software. From Equation 1, the tendency of TPS Pinnacle³ in predicting the interface doses were found, in addition to the obtained dose reduction degree on interface mass of static and dynamic phantom. For comparison, Equations 2 and 3 expresses the degree of underdose on mass interface as adopted below from Taylor et al [3];

$$\Delta D = \left(\frac{D_{measured} - D_{TPS}}{D_{TPS}} \right) \times 100 \% \quad (1)$$

$$R = \frac{D_{boundary}}{D_{ref}} \quad (2)$$

$$DRF = \frac{1}{4D_{ref}} (D_F + D_D + D_B + D_H) \quad (3)$$

where ΔD is dose discrepancy of interface point measurement ($D_{measured}$) to the TPS calculation (D_{TPS}). R is a ratio of the dose in the mass interface ($D_{boundary}$) to the dose at center mass (D_{ref}). R value less than 1 indicates that the interface areas is underdose to the center mass, while the R value of greater than 1 indicates that interface area is overdose to the center mass. Dose reduction factor (DRF) is the average of dose reduction in the mass interface. D_F , D_D , D_B , and D_H are interface dose point, shown in Figure 2.

3. Results and Discussion

3.1. Dose Distribution

The EBT3 film outputs using IDV software were shown in Figure 3 and Figure 4 for fast and slow CT technique, respectively. The white line described the GTV area of the simulated lung cancer which is also the interface area between cancer and lung tissue (Figure 2). The differences in the size of white lines in Figure 3 and 4 was caused by the difference in film size. Red color indicated the area of high doses. Figure 3a, Figure 4a, Figure 4b, Figure 4c and Figure 4d show that all of GTV area received a high dose, while not all areas of the GTV receiving high doses in dynamic phantom scanned using the

fast CT technique (Figure 3b, 3c and 3d)). The range of doses for each distribution is displayed in the histogram in each image.

Figure 3 shown that the GTV area of simulated cancer in a static phantom scanned using a fast CT technique received a dose in the range of 500 to 700 cGy, while the GTV area of cancer in a dynamic phantom received doses within range of 60 to 450 cGy. Such dose distribution caused the overall interface cancer of static phantom to receive high dose (in red area), while only upper cancer received high doses for the dynamic phantom. These dose distributions caused by the moving phantom effect that gave consequence to the accuracy of radiation beams to hit the target. The radiation beam can not be in the GTV region continuously. Figure 3b, c, and d shown that in the dynamic setup the radiation beam was more often exposed the upper part than the lower part of the mass.

For slow CT scanning technique, Figure 4 displayed the dose distribution in GTV area for static and dynamic run. In these Figures, it can be observed that the whole GTV area of the target is in the red region. The GTV area from slow CT technique received doses in the range of 500 to 750 cGy and 480 to 750 for static and dynamic setup, respectively. On slow CT technique, the overall interface of GTV has covered the high doses both for static and dynamic phantom condition. The situation is influenced by the cancer size differences of each scanning result. The cancer size of slow CT technique is larger compared to fast CT technique, especially for dynamic phantom. The result agrees with previous works; that images resulting from slow CT technique has larger target size than the target image from fast CT techniques [8], [9],[10], [11]. Larger target size kept the phantom inside the radiation beam along the dynamic movement. This, in turn, caused the cancer from slow CT technique to receive relatively high dose in all GTV area.

3.2. Interface Point Dose

Doses at the mass interface point were verified with TPS Pinnacle³ to identify the tendency of estimating interface dose. Table 1 and Table 2 shown the discrepancy of interface point dose for fast and slow CT techniques, respectively.

For fast CT scanning mode, Table 1 shown that TPS Pinnacle³ tended to estimate dose lower than the measured values for the static phantom condition, estimating higher interface doses than the measurement for all of phantom motion amplitudes for the dynamic phantom. On the other hand, slow CT scanning technique presented Table 2 which described that TPS tend to estimate dose lower than the measurements for static phantom condition, while the TPS tend presented the variation dose for each interface region at dynamic phantom.

For the phantom motion with amplitudes of 5 mm and 10 mm, the TPS estimates lower interface dose against measured values at the upper target; and higher estimation at the lower target area. In addition, the TPS estimated the point dose at interface area to be lower than measurement results for 20 mm amplitude of motion. From these result in *Tables 1* and *2*, it is seen that interface effect on TPS calculation was only identified in static phantom but it could not be identified in dynamic phantom. In dynamic phantom, motion effect was found to be more dominant than the interface effect.

In this work, an adaptive convolution algorithm estimated the interface dose to be lower than the measurement for both fast and slow CT for static phantom (0 mm motion amplitude). Previous studies by Shahine (1998) and Rosa (2010) reported that a simple dose calculation algorithm, like BATHO and ETAR algorithm, estimate the dose at interface area lower than the measurement up to 55% [1], [12]. However, Monte Carlo and collapsed cone convolution (CCC) showed a better result for estimating the dose at interface region [13]. Jones reported that CCC algorithm tend to estimate interface dose higher than Monte Carlo simulation results [14].

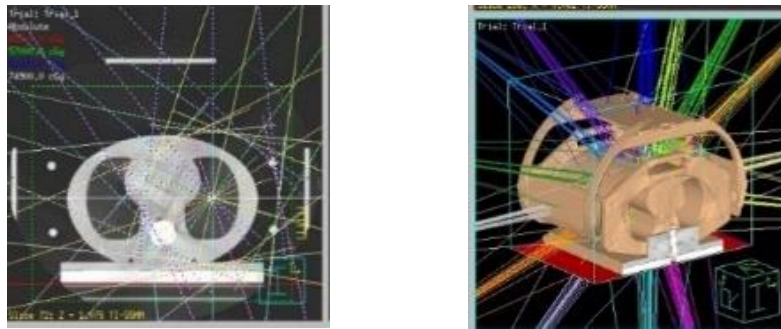


Figure 1. The position of lung cancer and SBRT planning

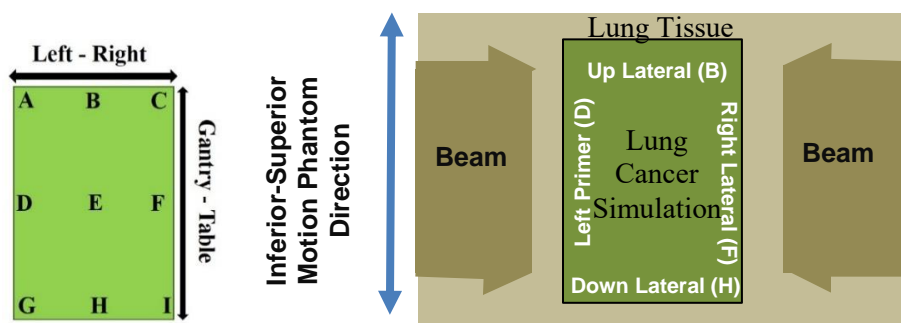


Figure 2. Illustration lung mass interface point measurement, beam direction and phantom motion direction

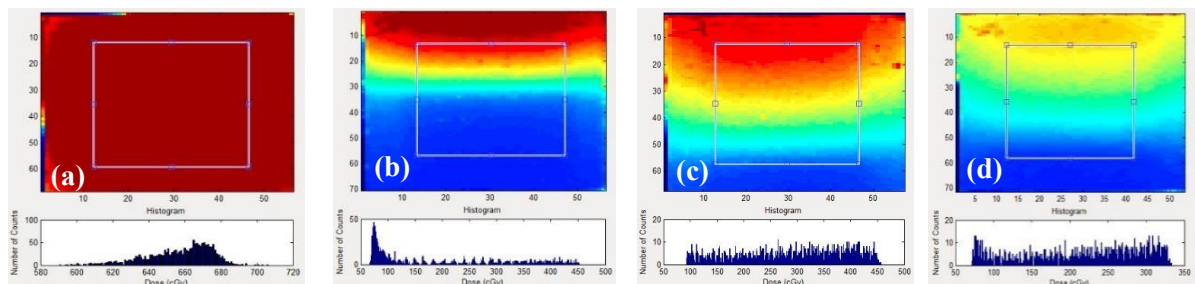


Figure 3. Dose distribution of lung mass (a) static and dynamic (b) 5 mm (c) 10 mm (d) 20 mm phantom amplitude fast CT technique

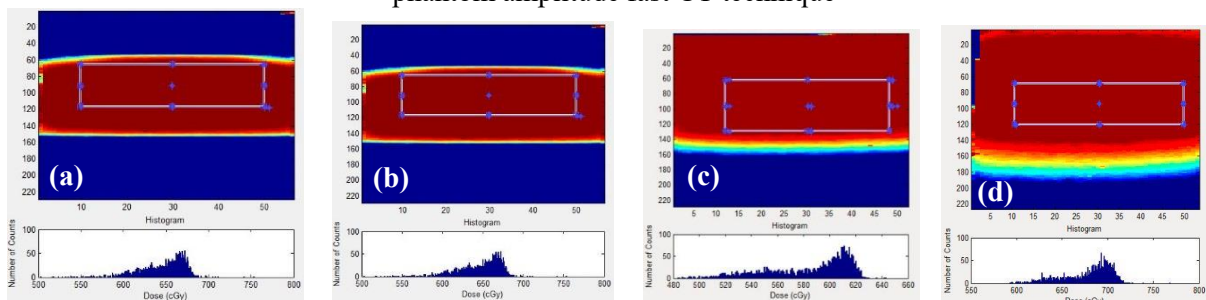


Figure 4. Dose distribution of lung mass (a) static and dynamic (b) 5 mm (c) 10 mm (d) 20 mm phantom amplitude slow CT technique

3.3. Dose Reduction Factor (DRF)

The dose of lung cancer interface decreased significantly, reaching up to 16% as seen in Table 3. Reduction of interface dose mostly occurred in the upper and lower lateral region of the simulated lesion.

In the fast CT scanning, the R value of dynamic phantom was more than unity (especially on the upper side of the lateral position), indicating that the area of lung mass interface received higher dose than the center of the mass area. The average dose reduction in the interface lung cancer was shown in Table 4. The relation between the amplitude of motion phantom and the average dose reduction was not found in this work.

Table 1. Discrepancy of Interface Point Dose for Fast CT Scanning

Interface Point	Discrepancy (ΔD) (%)			
	0 mm	5 mm	10 mm	20 mm
A	2.86	-12.47	-25.82	-43.39
B	1.40	-17.35	-23.01	-45.19
C	-1.67	-7.29	-13.25	-38.73
D	9.14	-78.10	-49.91	-62.63
E	1.27	-83.17	-49.86	-62.79
F	5.60	-78.44	-45.54	-60.86
G	3.14	-85.32	-81.11	-86.60
H	0.69	-86.52	-83.63	-88.42
I	5.04	-84.33	-79.59	-86.87

Table 2. Discrepancy of Interface Point Dose for Slow CT Scanning

Interface Point	Discrepancy (ΔD) (%)			
	0 mm	5 mm	10 mm	20 mm
A	3.55	7.18	6.22	35.59
B	13.85	5.76	7.22	37.48
C	4.05	8.59	19.41	36.14
D	0.45	5.56	0.43	9.81
E	0.16	-2.53	-1.68	13.52
F	1.22	-6.94	-1.99	7.57
G	7.80	-16.51	-9.58	15.21
H	11.85	-11.48	-5.47	15.56
I	12.42	-5.18	-1.52	15.20

Table 3. The ratio of interface dose to the centre mass dose (R)

Interface Point	Scanning Technique		Interface Point	Scanning Technique	
Right Primer Dose (F)	Fast CT	Slow CT	Up Lateral Dose (B)	Fast CT	Slow CT
0 mm	0.95	0.92	0 mm	0.94	0.86
5 mm	1.12	0.87	5 mm	4.45	0.92
10 mm	0.97	0.89	10 mm	1.46	0.99
20 mm	0.95	0.89	20 mm	1.44	0.98
Left Primer Dose (D)	Fast CT	Slow CT	Down Lateral Dose (H)	Fast CT	Slow CT
0 mm	0.97	0.90	0 mm	0.87	0.92
5 mm	1.19	0.96	5 mm	0.66	0.74
10 mm	0.91	0.91	10 mm	0.28	0.86
20 mm	0.94	0.89	20 mm	0.30	0.88

Table 4. Dose Reduction Factor (DRF)

Phantom Motion Amplitude (mm)	Fast CT	Slow CT
0	0.93	0.90
5	1.85	0.87
10	0.90	0.91
20	0.91	0.91

4. Conclusion

This work shown that the interface dose characteristics are influenced by scanning technique and phantom motion. For static phantom, fast CT scanning technique has smaller interface dose discrepancy than slow CT technique, while the slow CT scanning mode has smaller interface dose discrepancy than fast CT technique for dynamic phantom. On the other hand, calculation results from Pinnacle³ TPS implies that the dose of fast CT scanning was higher than measurement, with dose variation for slow CT scanning in dynamic phantom. Dose reduction of the interface cancer were up to 12% and 16% for static and dynamic phantom, respectively.

5. References

- [1] B. H. Shahine, M. S. . Al-Ghazi, and E. El-Khatib, "Exerimental evaluation of interface doses in the presence of air cavities compared with treatment planning algorithms," *Med. Phys.*, vol. 26, no. 3, pp. 350–355, 1998.
- [2] T. R. Mackie, E. El Khatib, J. Battista, J. Scrimger, J. Van Dyk, and J. R. Cunningham, "Lung dose corrections for 6 - and 15 - MV x rays," *Med. Phys.*, vol. 12, no. 327, 1985.
- [3] M. Taylor, L. Dunn, T. Kron, F. Height, and R. Franich, "Determination of peripheral underdosage at the lung-tumor interface using Monte Carlo radiation transport calculations," *Med. Dosim.*, vol. 37, no. 1, pp. 61–66, 2012.
- [4] A. I. Saito, J. G. Li, C. Liu, K. R. Olivier, and J. F. Dempsey, "Accurate heterogeneous dose calculation for lung cancer patients without high-resolution CT densities.," *J. Appl. Clin. Med. Phys.*, vol. 10, no. 2, p. 2847, 2009.
- [5] M. Miften, S. K. Das, I. J. Chetty, and D. Westerly, "Treatment Planning for Stereotactic Body Radiation Therapy," in *Stereotactic Body Radiation Therapy*, vol. 39, no. 1, 2012, pp. 91–113.
- [6] W. Van Elmpt, M. Öllers, M. Velders, K. Poels, B. Mijnheer, D. De Ruyscher, A. Dekker, P. Lambin, and L. Boersma, "Transition from a simple to a more advanced dose calculation algorithm for radiotherapy of non-small cell lung cancer (NSCLC): Implications for clinical implementation in an individualized dose-escalation protocol," *Radiother. Oncol.*, vol. 88, no. 3, pp. 326–334, 2008.
- [7] R. Boopathy, S. Padmanaban, V. Nagarajan, P. Sukumaran, P. Jeevanandam, S. Kumar, D. Rajasekaran, and L. A. Venkataraman, "Effects of Lung Tumor Motion on Delivered Dose Distribution during RapidArc Treatment Technique," *J. Med. Biol. Eng.*, vol. 30, no. 3, pp. 189–192, 2010.
- [8] D. Koste, F. J. Lagerwaard, R. H. Schuchhard-schipper, J. R. Van So, M. R. J. Nijssen-visser, P. W. J. Voet, S. S. Oei, and S. Senan, "Dosimetric consequences of tumor mobility in radiotherapy of stage I non-small cell lung cancer – an analysis of data generated using ‘ slow ’ CT scans," *Radiother. Oncol.*, vol. 61, pp. 93–99, 2001.
- [9] J. R. V. S. De Koste, F. J. Lagerwaard, H. C. J. De Boer, M. R. J. Nijssen-Visser, and S. Senan, "Are multiple CT scans required for planning curative radiotherapy in lung tumors of the lower lobe?," *Int. J. Radiat. Oncol. Biol. Phys.*, vol. 55, no. 5, pp. 1394–1399, 2003.
- [10] S. Seki, E. Kunieda, A. Takeda, T. Nagaoka, H. M. Deloar, T. Kawase, J. Fukada, O. Kawaguchi, M. Uematsu, and A. Kubo, "Differences in the definition of internal target volumes using slow CT alone or in combination with thin-slice CT under breath-holding conditions during

- the planning of stereotactic radiotherapy for lung cancer,” *Radiother. Oncol.*, vol. 85, no. 3, pp. 443–449, 2007.
- [11] K. Wurstbauer, H. Deutschmann, P. Kopp, and F. Sedlmayer, “Radiotherapy planning for lung cancer : Slow CTs allow the drawing of tighter margins,” *Radiother. Oncol.*, vol. 75, pp. 165–170, 2005.
- [12] L. A. R. Rosa, S. C. Cardoso, L. T. Campos, and V. G. L. Alves, “Percentage depth dose evaluation in heterogeneous media using thermoluminescent dosimetry,” *J. Appl. Clin. Med. Phys.*, vol. 11, no. 1, pp. 1–11, 2010.
- [13] M. R. Arnfield, C. H. Siantar, J. Siebers, P. Garmon, L. Cox, R. Mohan, C. H. Siantar, and L. Cox, “The impact of electron transport on the accuracy of computed dose,” vol. 1266, no. 2000, 2006.
- [14] A. O. Jones and I. J. Das, “Comparison of inhomogeneity correction algorithms in small photon fields,” *Med. Phys.*, vol. 32, no. 3, pp. 766–776, 2005.

Acknowledgements

This study was funded by Hibah PITTA Universitas Indonesia 2016 (contract number 2051/UN2.R12/HKP.05.00/2016). The authors would also like to acknowledge the help and assistance during the preparation and measurement process from medical physicists in the Department of Radiotherapy, Cipto Mangunkusumo General Hospital.